

Phenomenological theory of optical broadening in zero-dimensional systems applied to silicon nanocrystals

V. V. Nikolaev* and N. S. Averkiev
Ioffe Institute, St. Petersburg 194021, Russia

Minoru Fujii
Department of Electrical and Electronic Engineering,
Graduate School of Engineering, Kobe University, Kobe 657-8501, Japan
(Dated: April 6, 2016)

We develop a phenomenological theory of inhomogeneous broadening in zero-dimensional systems and apply it to study photoluminescence (PL) spectra of silicon nanocrystals measured at helium and room temperatures. The proposed approach allowed us to explain experimentally observed PL peak asymmetry, linear dependence of the peak width on its maximum and anomalous alteration of spectral characteristics with temperature increase.

Silicon nanocrystals (Si-NCs) embedded in a silicon dioxide matrix have been actively studied due to their potential for future-generation opto-electronics and photovoltaics¹. One of the advantageous features of Si-NCs is a significant dependence of optical properties on the nanocrystal size, which can provide tunability across a wide optical range. At the same time this leads to demand for Si-NC size control²⁻⁴ for device applications.

A typical PL spectrum of a Si-NC ensemble exhibits a broad peak with the width between 100 and 400 meV even at helium temperatures⁵⁻⁷, whereas single Si-NCs at low temperatures demonstrate narrow a few-meV-wide emission lines⁸. It may be expected that the PL peak broadening is related to the NC size dispersion^{7,9,10} through the size dependence of the optical-transition energies. However, finding the exact relation between NC size and optical-transition energy is a difficult task due to complex structural properties of Si-NCs in silicon dioxide surrounding^{11,12}. Additionally, the mechanism of the radiative recombination in Si-NCs is not yet thoroughly understood¹²⁻¹⁵.

In this Letter we develop a general phenomenological theory of inhomogeneous broadening in zero-dimensional systems which does not rely on a particular microscopic model of choice, and we apply it to interpret our experimental results on Si-NC ensembles.

Let us suppose that there is a one-to-one correspondence between the energy E of a particular optical transition and NC size parameter d , which is represented by a smooth function $E = f(d)$. If the NC size dispersion in an ensemble is described by a distribution function $P(d)$ then the density of optical transitions (DoOT) per energy interval $\rho(E)$ is proportional to⁹

$$\rho(E) \propto P(f^{-1}(E)) \left| \frac{df^{-1}(E)}{dE} \right|, \quad (1)$$

where $d = f^{-1}(E)$ is the inverse of $E = f(d)$.

The function $f(d)$ is defined by structural and material properties of nano-objects and is generally unknown. Here, similarly to our previous work¹⁶, we presume that in a certain interval of the NC size variation the micro-

scopic size dependence can be approximated by a power function¹³ (PF)

$$E = f(d) = \frac{A}{d^\gamma} + \tilde{E}_g, \quad (2)$$

where $A > 0$, $\gamma > 0$ and \tilde{E}_g are phenomenological parameters. In this Letter we consider size dispersion described by the asymmetric log-normal (LN) distribution^{9,17,18}

$$P_{LN}(d) = \frac{1}{d\sigma\sqrt{2\pi}} \exp\left(-\frac{1}{2\sigma^2} \left[\ln\left(\frac{d}{\bar{d}}\right)\right]^2\right). \quad (3)$$

Here \bar{d} is the median of the distribution, and σ defines the relative standard deviation $\delta d/d_{av} = \sqrt{\exp(\sigma^2) - 1}$ of the size parameter d from its average value $d_{av} = \bar{d} \exp(\sigma^2/2)$. Observation of LN distributions has been reported in many systems of nano-objects¹⁸, including ensembles of Si-NCs^{2-4,9,19-21}.

Substitution of Eqs. (2,3) into rhs of Eq. (1) produces a new normalized asymmetric distribution ($E > \tilde{E}_g$)

$$P_{PF-LN}(E) = \frac{\exp\left(-\frac{1}{2\chi^2} \left[\ln\left(\frac{E-\tilde{E}_g}{\bar{E}-\tilde{E}_g}\right)\right]^2\right)}{\chi(E-\tilde{E}_g)\sqrt{2\pi}}, \quad (4)$$

where $\chi = \gamma\sigma$; \bar{E} is the median of the transition-energy distribution directly connected to the median size \bar{d} by means of PF Eq. (2): $\bar{E} = f(\bar{d}) = A/\bar{d}^\gamma + \tilde{E}_g$.

Similarly to the size-dispersion parameter σ in the LN distribution Eq. (3), χ defines the asymmetry of the peak and the relative standard deviation of the “effective quantized energy” $\varepsilon = E - \tilde{E}_g$ from its average value $\varepsilon_{av} = E_{av} - \tilde{E}_g$ through the expression $\delta\varepsilon/\varepsilon_{av} = \delta E/(E_{av} - \tilde{E}_g) = \sqrt{\exp(\chi^2) - 1}$. Here E_{av} is the average transition energy.

The full width at half maximum (FWHM) of the peaked distribution function P_{PF-LN} can be expressed in an analytical form:

$$\Delta E = 2 \left(E_{max} - \tilde{E}_g \right) \text{sh} \left(\chi \sqrt{2 \ln(2)} \right), \quad (5)$$

where E_{max} is the peak energy (mode) of the $PF-LN$ distribution. As can be seen from this expression, the peak broadens with the increase of the parameter χ . Since χ is the product of σ (which characterizes the relative width of a size distribution) and the exponent γ , we naturally arrive at the conclusion that the width and the asymmetry of the DoOT peaks depend on the size dispersion as well as on the character of the transition-energy dependence on size. We note that $P_{PF-LN}(E)$ Eq. (4) approaches the Gaussian distribution when $\chi \rightarrow 0$.

Eq. (5) can be rewritten in the following form

$$\Delta E = 2 \exp(-\chi^2) \operatorname{sh}\left(\chi \sqrt{2 \ln(2)}\right) \frac{A}{d^\gamma}, \quad (6)$$

to reveal that, at constant level of size dispersion set by σ , the FWHM of an inhomogeneously-broadened optical transition will increase with the decrease of the median NC size \bar{d} , and the character of FWHM dependence on size will follow the power law described by the same exponent γ which defines the transition energy dependence.

We argue that the DoOT in the form of Eq. (4) can be used to model the experimental PL spectra of silicon nanocrystals. Indeed, if the redistribution of electrons and holes between NCs is prohibited by high potential barriers, variations of the pump-radiation absorption and internal quantum efficiency²² across an ensemble are slow then the PL intensity at a certain photon energy will be defined by the number of NCs with the related optical-transition energy, i.e. PL spectra will replicate the shape of the DoOT. In this work we neglect the dependence of the internal quantum efficiency on size justifying it by the results of experimental investigations which show that, despite the strong reduction of the radiative lifetime with the NC size decrease evident from time-resolved experiments^{6,22}, internal quantum efficiency varies moderately, especially in the long wavelength range for the samples with relatively large NCs²².

In Fig. 1 PL spectra measured at helium and room temperatures (RT) are displayed alongside diameter distributions in five Si-NC/SiO₂ samples under investigation. The PL experiments were conducted at a low excitation power density of 4 mW/cm², in order to avoid NC ground level saturation and related effects. Experimental histograms, obtained by high-resolution transmission electron microscopy (TEM), were fitted by scaled LN distributions (see Fig. 1(c)); the size-dispersion parameter σ was found close to $\sigma_{TEM} \approx 0.2$ in all five samples. Information on the sample preparation and experimental setup can be found in Ref. 6.

The measured temperature dependence of PL decay time for these samples⁶ was successfully described by the two-level Calcott's model²³. The model assumes that PL at low temperatures originates from a ground “semi-dark” exciton level, which is predominantly spin-triplet with moderate admixture of spin-singlet character facilitated by the spin-orbit interaction. Our measurements at 4 K (Fig.1(a)) show an additional peak associated with P_b centers at Si/SiO₂ interface²⁴. At RT PL is domi-

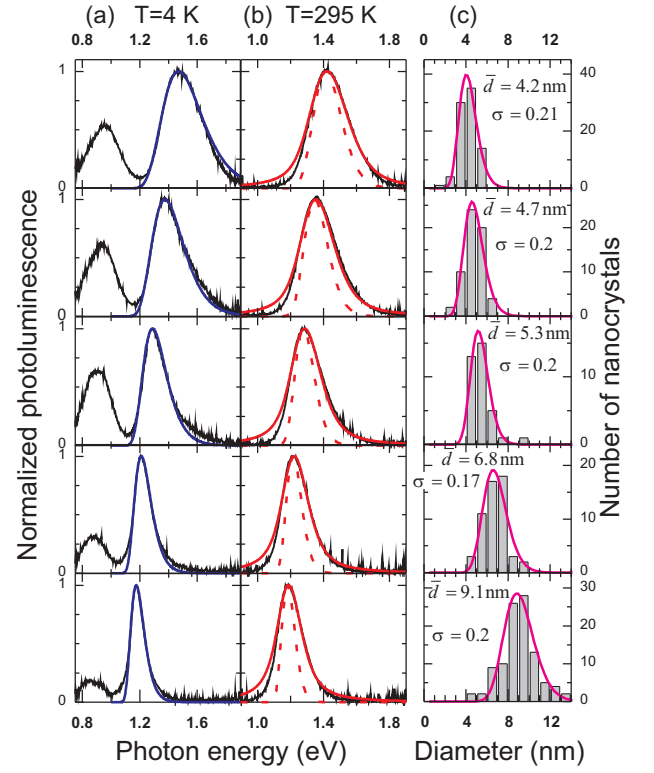


FIG. 1. (Color online) Measured and calculated PL spectra at T=4 K (a) and T=295 K (b) from five samples with different NC size distributions (shown in (c)). Spectra are normalised to their maximum intensities; dashed curves in (b) show modelled RT spectra without homogeneous broadening.

nated by recombination of an excited “semi-bright” exciton level which is split from “semi-dark” level by the electron-hole exchange interaction²³ and has mainly spin-singlet character. The main PL peaks at both temperatures demonstrate significant degree of asymmetry alongside with the blueshift and linewidth broadening with the decrease of NC size.

Measurements on single Si-NCs show⁸ that at cryogenic temperatures the homogeneous broadening of an emission line is less than 3 meV and, therefore, at T=4 K it can be safely neglected compared to peak widths exceeding 100 meV observed in our experiments. In this case Eq. (4) and related equations can be used directly to model experimental data at T=4 K, provided the assumptions listed above are valid.

Figure 2(a) shows the FWHM ΔE of the main PL peaks from Fig. 1(a,b) as functions of peak energies E_{max} . Experimental points lay close to straight lines. Analysis of Eq. (5) reveals that linear dependence can take place when PF Eq. (2) describes transition energies in all five samples and NC diameters are distributed log-normally with an approximately equal value of the size-dispersion parameter σ . The values of phenomenological parameters for T=4 K $\bar{E}_{g4K} = 1.026 \pm 0.013$ eV and $\chi_{4K} = 0.31 \pm 0.02$ are obtained straightforwardly by fitting the linear dependence Eq. (5) to the experimental

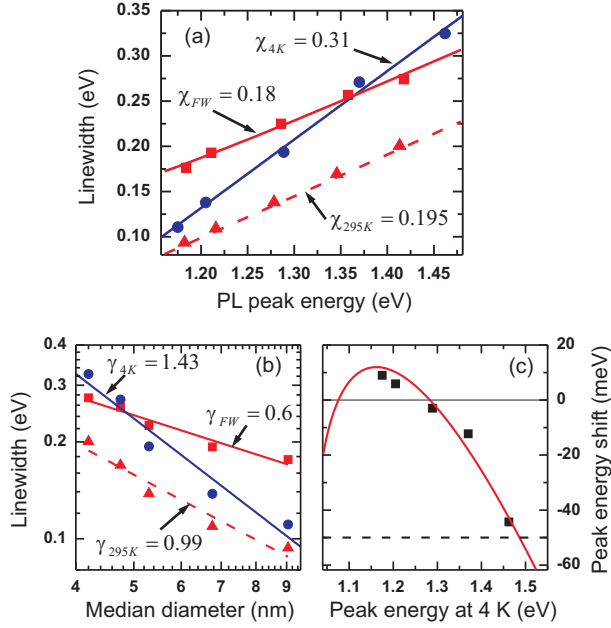


FIG. 2. (Color online) (a,b) PL FWHM measured at T=4 K (blue circles), T=295 K (red squares) and extracted inhomogeneous linewidths for T=295 K (red triangles) as functions of PL peak energy E_{max} (a) and NC median diameter \bar{d} (b) (note log-log scale in (b)). (c) Energy shift of the PL peak E_{max} with the temperature increase from 4 K to 295 K as function of E_{max} at 4 K. Lines in (a-c) represent modelling.

data. These values were used to model the PL spectra with the scaled functions $P_{PF-LN}(\bar{E}, \chi_{4K}, \tilde{E}_{g4K}; E = \hbar\omega)$, Eq. (4), where median energies \bar{E} (which are close to the PL peak energies) are found by fitting. In Fig. 1(a) a good agreement between calculated and experimental data can be seen, with the modelled spectra perfectly replicating the asymmetry and the linewidth variation of the measured PL peaks.

In Fig. 2(b) FWHM values are plotted as functions of the NC median diameter. According to our model (see Eq. (6)) this dependence should be close to linear in log-log scale, and the slope of the line gives the value of the exponent ($\gamma_{4K} = 1.4 \pm 0.2$ for T=4 K). The extracted parameters allow us to estimate the level of size dispersion from PL spectra alone $\sigma = \chi_{4K}/\gamma_{4K} \approx 0.22$ approximately matching TEM results. Additionally, the dependence of the retrieved median effective quantized energies $\bar{\varepsilon} = \bar{E} - \tilde{E}_g$ on median diameter, plotted in log-log scale (not shown), is approximately linear, which is in accordance with Eq. (2); and the obtained absolute value of the slope 1.4 ± 0.2 equals the previous result for γ_{4K} . These findings suggest that the presented theoretical approach is consistent with the experimental results at T=4 K.

The retrieved value of exponent γ_{4K} agrees well with $\gamma = 1.39$ calculated by Delerue¹³ *et al.*. The effective bandgap $\tilde{E}_{g4K} \approx 1.025$ eV is smaller than the bandgap of crystalline Si (1.17 eV), which is possibly partly due

to an effective hydrostatic pressure²⁵ related to the NC surface¹⁹, the energy of an emitted optical phonon²⁶ and the bulk-exiton binding energy. In addition, \tilde{E}_{g4K} may differ from the value of the material bandgap because the formula Eq. (2) approximates the transition energy dependence only in a limited diameter range.

Comparing the PL spectra measured at 4 K and 295 K one may find some unexpected effects. Firstly, the FWHM growth with the increase of PL peak energy (Fig. 2(a)) or decrease of NC size (Fig. 2(b)) is less steep at RT. More surprisingly, the two samples with the smallest NCs ($\bar{d} = 4.2$ and 4.7 nm) demonstrate PL peak narrowing with the increase of the temperature (see Fig. 2(b)). The shift of the PL peak energy with the temperature increase is plotted in Fig. 2(c) as function of the peak energy at 4 K. One can see that the two samples with smallest PL peak energies (and largest median NC diameters $\bar{d} = 6.8$ and 9.1 nm) exhibit blueshift with the temperature increase. This is a counter-intuitive behaviour since the corresponding Si bandgap reduction is approximately 50 meV (shown by a dashed line in Fig. 2(c)) Saturation of NC ground levels at 4 K cannot serve as an explanation for such blueshift, since it has the opposite effect²⁷.

An attempt to directly apply the approach used for T=4 K to the experimental results at T=295 K leads to the following contradiction. Fitting the linear dependence Eq. (5) to the experimental FWHM in Fig. 2(a) gives $\chi_{FW} = 0.18 \pm 0.01$ and an unexpectedly low value for the effective bandgap $E_{gFW} = 0.75 \pm 0.03$ eV; application of Eq. (6) to the measured data (red squares in Fig. 2(b)) produces the value of exponent $\gamma_{FW} = 0.6 \pm 0.08$ leading to the estimate of the size-dispersion parameter $\sigma = \chi_{FW}/\gamma_{FW} \approx 0.3$ which exceeds the experimentally obtained $\sigma_{TEM} \approx 0.2$ by half.

This contradiction occurred because homogeneous broadening of Si-NC optical transitions was not accounted for by the analysis above. Experiments show^{8,28} that single Si-NCs exhibit quite large PL linewidths (100-150 meV) at RT. Manifestation of homogeneous broadening of more than 100 meV was also seen in ensemble investigations²⁶.

To account for homogeneous broadening we convolute DoOT given by $P_{PF-LN}(E)$ Eq. (4) with the Lorentzian function $L(E) = 2\Gamma_{hom}/[\pi(4E^2 + \Gamma_{hom}^2)]$, where Γ_{hom} is the FWHM of a single-NC transition. It was found that the best fit to experimental data can be achieved if $\Gamma_{hom} = 130$ meV is used, which is in accordance with reported measurements²⁸. The parameters $\chi_{295K} \approx 0.195$ and $\tilde{E}_{g295K} \approx 0.98$ eV were chosen to match the measured RT FWHM in Fig. 2(a). The resulting spectra simulations are shown in Fig. 1(b) demonstrating good agreement with experiment. Slight overestimation of PL intensity in the low-photon-energy region might be due to the deviation of the actual size dependence from PF Eq. (2) for larger NCs.

The value of the exponent $\gamma_{295K} = 0.99 \pm 0.13$ can be derived from the dependence of the obtained inhomoge-

neous part of the linewidth on NC size (Fig. 2(b), red triangles). The size dependence of the median effective quantized energies $\bar{\varepsilon} = \bar{E} - \bar{E}_{g295K}$ (not shown) produces the same value of exponent. The ratio $\chi_{295K}/\gamma_{295K} \approx 0.2$ coincides with σ_{TEM} , which shows that our model is consistent.

Now an explanation to the anomalous PL linewidth narrowing and blueshift with temperature increase can be proposed. With elevation of the temperature from 4 K to 295 K the dominant luminescence channel switches from recombination of semi-dark lower exciton states to upper semi-bright states, and the energy dependence on size of semi-bright states at RT differs from that of semi-dark states at 4 K. Both dependencies can be approximated by Eq. (2) but with remarkably different parameters. Effective bandgap \bar{E}_g shrinks from approximately 1.025 eV to 0.98 eV, which is in line with the Si bandgap reduction by 50 meV. The other two phenomenological parameters change as follows: $\gamma_{4K} \approx 1.4$ to $\gamma_{295K} \approx 1.0$ and $A_{4K} \approx 3.3 \text{ eVnm}^{1.4}$ to $A_{295K} \approx 1.8 \text{ eVnm}$ (values of A are obtained by fitting Eq. (6) to experimental data in Fig. 2(b)).

Decrease in the value of the exponent γ means that the variation of the optical-transition energy with the NC size becomes slower, which leads to the reduction of the inhomogeneous broadening with temperature increase (compare blue and dashed red lines in Figs. 2(a,b)). The thermal broadening of a single-NC transition leads to the increase of the total peak width by 70-80 meV, which partly compensates the decrease of inhomogeneous broadening. For samples with small NC sizes the decrease of inhomogeneous broadening is most pronounced, and the homogeneous broadening is unable to compensate it, resulting in the total linewidth narrowing with temperature elevation.

We calculated the difference between PL peak maxima at 4 K and 295 K using phenomenological parameters listed above (continuous red line in Fig. 2(c)); the size-

dispersion parameter was set to $\sigma = 0.2$. One can see that the modelling reproduces the anomalous blueshift for structures with larger NC diameters. The origins of this effect are as follows. Firstly, the semi-bright state at 295 K approaches bandgap with the size increase more slowly than the semi-dark state at 4 K, which is due to γ reduction. At certain interval of (comparatively large) NC diameters semi-bright transition energies at T=295 slightly exceed semi-dark transition energies at 4 K despite the reduced RT effective bandgap \bar{E}_{g295K} (45 meV smaller than \bar{E}_{g4K}). Secondly, enhancement of thermal broadening blueshifts the PL peak by 5-10 meV.

Significant reduction of γ with temperature rise indicates that physical properties of Si-NCs in SiO_2 matrix strongly differ from those of homogeneous crystalline Si. The mechanism which leads to γ alteration may be due to complex effects which temperature elevation imposes on stress profiles²⁹, the transition region between a Si core and SiO_2 matrix^{11,12} or defect/surface states¹⁴, and still needs to be clarified. It should be noted that, according to experimental observations, for smaller Si-NCs in SiO_2 matrix the blueshift with the size reduction is quenched and the PL peak energy normally does not exceed 1.8-2.0 eV. From this one may conclude that the divergent PF Eq. (2) will not adequately describe NCs with small diameters and, therefore, our method is not applicable to such samples.

In conclusion, employing log-normal size distribution^{17,18} we developed a concise phenomenological theory of inhomogeneous broadening in zero-dimensional systems which contains few fitting parameters. Obtained analytical expressions allow for relatively straightforward interpretation of experimental results. The proposed approach clarifies the measured line shape and linewidth variations of the PL spectra of silicon nanocrystals. We explain anomalous PL line narrowing and blueshift with temperature increase by competition between opposite variations of homogeneous and inhomogeneous broadening and by modification of the transition-energy size dependence.

* valia.nikolaev@gmail.com

- ¹ F. Priolo, T. Gregorkiewicz, M. Galli, and T. F. Krauss, *Nature Nanotech.* **9**, 19 (2014).
- ² M. Zacharias, J. Heitmann, R. Scholz, U. Kahler, M. Schmidt, and J. Blasing, *Appl. Phys. Lett.* **80** (2002).
- ³ J. Laube, S. Gutsch, D. Hiller, M. Bruns, C. Kbel, C. Weiss, and M. Zacharias, *J. Appl. Phys.* **116**, 223501 (2014).
- ⁴ B. Han, Y. Shimizu, G. Seguíni, E. Arduca, C. Castro, G. Ben Assayag, K. Inoue, Y. Nagai, S. Schamm-Chardon, and M. Perego, *RSC Adv.* **6**, 3617 (2016).
- ⁵ Y. Kanzawa, T. Kageyama, S. Takeoka, M. Fujii, S. Hayashi, and K. Yamamoto, *Solid State Commun.* **102**, 533 (1997).
- ⁶ S. Takeoka, M. Fujii, and S. Hayashi, *Phys. Rev. B* **62**, 16 820 (2000).

- ⁷ C. Meier, A. Gondorf, S. Lüttjohann, A. Lorke, and H. Wiggers, *J. Appl. Phys.* **101**, 103112 (2007).
- ⁸ I. Sychugov, R. Juhasz, J. Valenta, and J. Linnros, *Phys. Rev. Lett.* **94**, 087405 (2005).
- ⁹ H. Yorikawa and S. Muramatsu, *Appl. Phys. Lett.* **71**, 644 (1997).
- ¹⁰ P. F. Trwoga, A. J. Kenyon, and C. W. Pitt, *J. Appl. Phys.* **83**, 3789 (1998).
- ¹¹ N. Daldosso, M. Luppi, S. Ossicini, E. Degoli, R. Magri, G. Dalba, P. Fornasini, R. Grisenti, F. Rocca, L. Pavesi, S. Boninelli, F. Priolo, C. Spinella, and F. Iacona, *Phys. Rev. B* **68**, 085327 (2003).
- ¹² M. Luppi and S. Ossicini, *Phys. Rev. B* **71**, 035340 (2005).
- ¹³ C. Delerue, G. Allan, and M. Lannoo, *Phys. Rev. B* **48**, 11024 (1993).
- ¹⁴ S. Godefroo, M. Hayne, M. Jivanescu, A. Stesmans,

- M. Zacharias, O. I. Lebedev, G. Van Tendeloo, and V. V. Moshchalkov, *Nature Nanotech.* **3**, 174 (2008).
- ¹⁵ W. D. A. M. de Boer, D. Timmerman, T. Gregorkiewicz, H. Zhang, W. J. Buma, A. N. Poddubny, A. A. Prokofiev, and I. N. Yassievich, *Phys. Rev. B* **85**, 161409 (2012).
 - ¹⁶ V. V. Nikolaev and N. S. Averkiev, *Appl. Phys. Lett.* **95**, 263107 (2009).
 - ¹⁷ E. Limpert, W. A. Stahel, and M. Abbt, *BioScience* **51**, 341 (2001).
 - ¹⁸ R. Espiau de Lamaestre and H. Bernas, *Phys. Rev. B* **73**, 125317 (2006).
 - ¹⁹ I. F. Crowe, M. P. Halsall, O. Hulko, A. P. Knights, R. M. Gwilliam, M. Wojdak, and A. J. Kenyon, *J. Appl. Phys.* **109**, 083534 (2011).
 - ²⁰ I. Dogan and M. C. M. van de Sanden, *J. Appl. Phys.* **114**, 134310 (2013).
 - ²¹ J. Laube, S. Gutsch, D. Wang, C. Kbel, M. Zacharias, and D. Hiller, *Appl. Phys. Lett.* **108**, 043106 (2016).
 - ²² S. Miura, T. Nakamura, M. Fujii, M. Inui, and S. Hayashi, *Phys. Rev. B* **73**, 245333 (2006).
 - ²³ P. D. J. Calcott, K. J. Nash, L. T. Canham, M. J. Kane, and D. Brumhead, *J. Phys.: Condens. Matter* **5**, L91 (1993).
 - ²⁴ M. Fujii, A. Mimura, S. Hayashi, K. Yamamoto, C. Urakawa, and H. Ohta, *J. Appl. Phys.* **87**, 1855 (2000).
 - ²⁵ X. Zhu, S. Fahy, and S. G. Louie, *Phys. Rev. B* **39**, 7840 (1989).
 - ²⁶ M. Fujii, D. Kovalev, B. Goller, S. Minobe, S. Hayashi, and V. Y. Timoshenko, *Phys. Rev. B* **72**, 165321 (2005).
 - ²⁷ A. M. Hartel, S. Gutsch, D. Hiller, and M. Zacharias, *Phys. Rev. B* **85**, 165306 (2012).
 - ²⁸ J. Valenta, R. Juhasz, and J. Linnros, *Appl. Phys. Lett.* **80**, 1070 (2002).
 - ²⁹ K. Kleovoulou and P. C. Kelires, *Phys. Rev. B* **88**, 085424 (2013).